Journal of Atmospheric and Solar–Terrestrial Physics 277 (2025) 106673

Contents lists available at ScienceDirect

Journal of Atmospheric and Solar–Terrestrial Physics

journal homepage: www.elsevier.com/locate/jastp

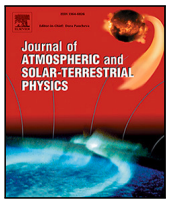

Research paper

Mean-field dynamo and forecasting of solar activity

Vladimir Obridko [a], Antonina Shibalova [a,1], Dmitry Sokoloff [a,b,*,1], Ilya Livshits [a,1]

[a] IZMIRAN, Kaluzhskoe Shosse 4, Moscow, 108840, Russia
[b] Department of Physics and Center for Fundamental and Applied Mathematics, Lomonosov Moscow State University, Leninskie gory 1, Moscow, 119991, Russia

ARTICLE INFO

Dataset link: http://wso.stanford.edu/synopticl.html

Keywords:
Solar cycle
Mean-field dynamo
Solar activity waves

ABSTRACT

According to the generally accepted theory, the field of local active areas arises from the poloidal magnetic field. The field in the polar regions, which is measured directly by magnetographs, can be a proxy for the latter. It has been shown that the mean-field dynamo is undoubtedly the main mechanism that generates solar activity and the 11-year cycle. However, the magnetic flux generated in the dynamo, although it is the genetic basis of solar activity, still does not allow us to unambiguously connect the characteristics of the magnetic field with other indices of solar activity, including the best known indicator, the number of sunspots. Magnetic fields of active regions and spots are formed from the mean magnetic flux. Its most important properties are the threshold nature and the preservation of the full flux. This is why a completely reliable long-term SSN forecast is possible after the occurrence of an equatorial wave approximately 18 months before the maximum. The processes in leptocline play a decisive role in this case.

1. Introduction

According to the generally accepted theory, the fields of local regions arise from the poloidal magnetic field. A proxy for the latter can be the field in the polar regions that is measured directly by magnetographs. It is true that these measurements are not very accurate, since the field at the pole is mainly perpendicular to the line of sight and, therefore, magnetographs give a large error. However, until now, the available data showed a high correlation between the magnitude of the polar field and the number of sunspots (Wang and Sheeley, 2009; Petrovay, 2020; Biswas et al., 2023).

This view relies on the idea that there is a single mechanism of solar activity generation and that once the poloidal field is formed, the sunspot cycle is completely predetermined. This is not always the case. It is not clear to what extent the solar dynamo is determined by stochastic or deterministic processes (Mininni et al., 2002). Furthermore, existing dynamo models deal with mean-field dynamos. Therefore, the output of any theory is the field structure, not the sunspot number that should be predicted. As a result, attempts to rely on dynamo models have yielded contradictory results (Biswas et al., 2023; Bushby and Tobias, 2007; Kitiashvili and Kosovichev, 2008, 2011; Kitiashvili, 2016; Dikpati et al., 2006; Dikpati and Gilman, 2006; Choudhuri et al., 2007; Upton and Hathaway, 2018; Jiang et al., 2018, 2023; Bhowmik and Nandy, 2018; Labonville et al., 2019; Guo et al., 2021; Bhowmik et al., 2023). For a detailed review of these publications, see Nandy (2021). In this regard, the current cycle is indicative. According to polar field data, one would expect the cycle to be almost the same as Cycle 24 or slightly higher (Nandy, 2021).

In May 2023, the smoothed SSN number reached 123.9 and continued to rise steadily. Cycle 25 promised to be at least 10% higher than Cycle 24 (Obridko et al., 2023b,a) as the arrow in Fig. 1 shows, but this forecast also turned out to be underestimated. A strong increase in activity in the second half of 2024 changed the course of the cycle and the smoothed value for March 2024 was 141.3. Currently, according to the ROB forecast service (https://sidc.be/SILSO/forecasts), the maximum is expected in October 2024, and its height will be about 160.

2. Cyclic variation of the magnetic field at all latitudes

To understand the nature of the anomalous cycle, we must first look at the cyclic variation of solar activity at all latitudes.

This rather complex supersynoptic map of the magnetic field (Fig. 2) allows us to identify the manifestations of the following processes. We see an area where the flow migrates to the poles from about −35° and +35° in the southern and northern hemispheres, respectively. This phenomenon, commonly called Rush-to-the-Poles (RTP), is mainly associated with large-scale magnetic fields. For example, in 2020 (when a

* Corresponding author at: Department of Physics and Center for Fundamental and Applied Mathematics, Lomonosov Moscow State University, Leninskie gory 1, Moscow, 119991, Russia.
E-mail addresses: obridko@mail.ru (V. Obridko), as.shibalova@physics.msu.ru (A. Shibalova), sokoloff.dd@gmail.com (D. Sokoloff), ilivsh@gmail.com (I. Livshits).
[1] These authors contributed equally to this work.

https://doi.org/10.1016/j.jastp.2025.106673
Received 4 June 2025; Received in revised form 11 October 2025; Accepted 28 October 2025
Available online 4 November 2025

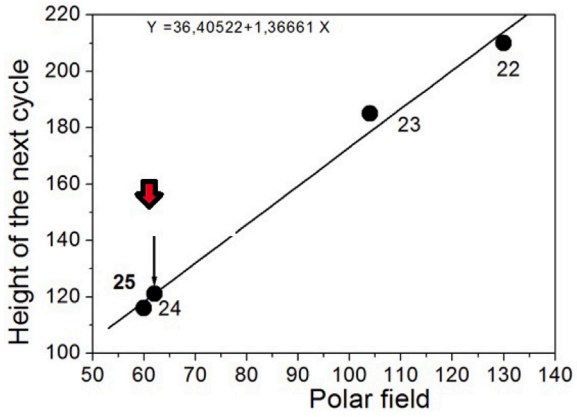

Fig. 1. Relationship between the polar field measured in μT and the height of the upcoming sunspot cycle. For cycle 25, two values are shown - the one predicted based on the polar field (thin arrow) and the one actually achieved in October 2024 (thick red arrow)

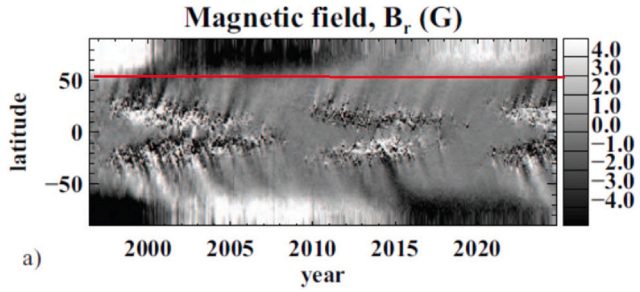

Fig. 2. The magnetic time-latitude ("butterfly") diagram for the radial component of the line-of-sight magnetic field from the SOHO and SDO data; picture is taken from Rozelot et al. (2025). Red line is added by us to show the region where the polar field is measured.

forecast of the polar field for Cycle 25 was issued), we see a long bright band (i.e. a long-lived, slightly changing field of positive polarity) near the north pole, which comes to the pole from the mid-latitudes. At the same time, a gray band of negative polarity appears in the mid-latitudes, which begins to drift toward the pole and reaches it only in 2024. After the RTP reaches the pole, it replaces the previous wave of activity, leading to a reversal of the magnetic field. At the same time, a third band of intermittent color appears (mostly black as at the pole). This wave drifts toward the equator and reaches it only by 2025. The wave appears as a standard Maunder butterfly diagram and is primarily associated with the local magnetic fields of active regions. Both the pole and the equatorial waves appear almost simultaneously and have opposite dominant polarities of the magnetic field. However, the point is that at certain times the map shows two Rush-to-the-Poles waves with opposite magnetic field polarities. When one of them almost reaches the pole, the other one just appears at mid-latitudes. At these times, the map contains three areas of the field polarity which are opposite in a given zone to the neighboring one. In the southern hemisphere the picture is identical up to the change of sign.

The simultaneous presence of two Rush-to-the-Poles events with opposite magnetic-field polarities on the Sun has attracted the attention of experts. In particular, McIntosh et al. (2014, 2019, 2020, 2021) introduced the concept of a cycle terminator as the moment when two activity waves depart from the latitude of 55°, one propagating equatorward and the other poleward. Obridko et al. (2023b,a) expanded

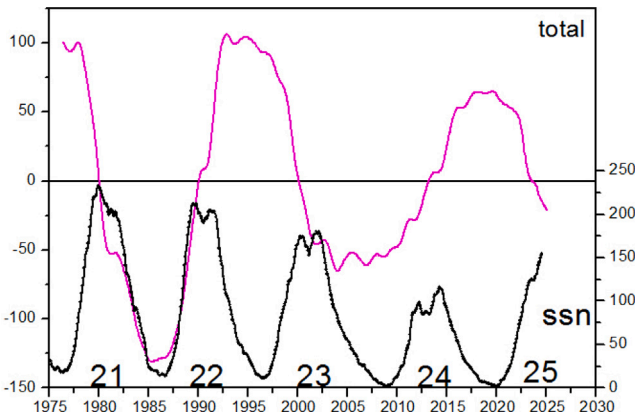

Fig. 3. Polar field measured (http://wso.stanford.edu/Polar.html) - magenta line and sunspot number - black line.

this concept. According to their proposal, it includes the simultaneous propagation of all three coexisting activity waves (two poleward and one drifting equatorward). This lasts for about a year. This time interval is called the "overlap phase". This overlap phase can be quantitatively described in terms of the 5th zonal harmonic of the magnetic field.

Using the Hilbert transform, McIntosh et al. (2020) calculated terminator times over 140 years with an accuracy of 0.01 years. In particular, after 1978, the terminators occurred at 1978.00, 1988.25, 1998.25, and 2011.08. The data are quite close to the times of our overlapping phases. McIntosh et al. (2020) proposed using the time between two successive terminators as a predictor of the solar cycle amplitude and expected Cycle 25 to be very high. However, this idea requires that the terminators were determined with very high accuracy, which is generally quite difficult.

3. What is meant by the polar field?

Why did the forecast of the height of Cycle 25 based on the polar field data not work? An important point here is that the data available from the WSO website (http://wso.stanford.edu/Polar.html) are not exactly the polar field (of course, there are other obvious limitations).

The Sun's Polar Field strength is measured in the polemost 3' apertures at WSO each day. The polemost aperture measures the line-of-sight field between about 55° and the poles. In this case, the longitudinal component is measured directly, i.e. at these latitudes it is close to the meridional one. Even if we assume that the field on the photosphere is radial, then at these latitudes it is multiplied by the cosine of the latitude, which is < 0.57. In Fig. 2, the lower limit of the summation interval is shown with the red line. It is evident that the field structure here is far from simple. Both waves traveling to the pole contribute to it, and the contribution of the field near the lower boundary is dominant.

Fig. 3 shows the polar field based on data from http://wso.stanford.edu/Polar.html (magenta line) and the smoothed sunspot number SSN based on data from https://sidc.be/SILSO/datafiles. It is evident that the SSN maxima correspond fairly well to the reversals of the polar magnetic field. At the same time, the SSN minima correlate poorly with the dates of the polar field maxima. For example, in 1994 and 2004 the lead of the latter is quite significant. Moreover, the date and magnitude of the polar field extremum are very uncertain. It is understandable since, as can be seen in Fig. 2, this extremum is the sum of three waves of different polarity and different dependence on time and latitude.

This means that one should not focus on the polar field. The model must include a scheme for converting the mean field into spots and take into account that this occurs somewhat differently in the two hemispheres and, probably, directly under the photosphere.

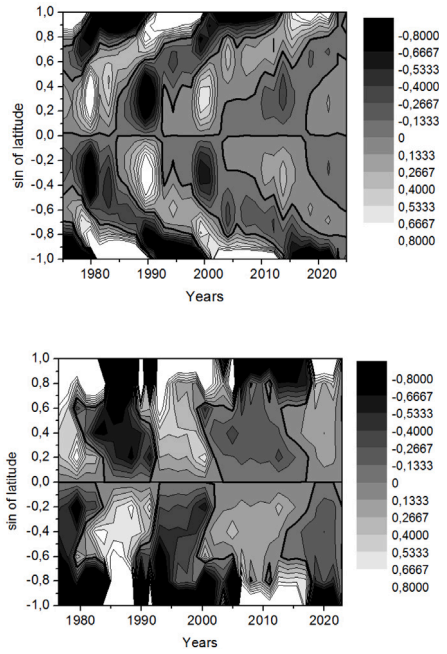

Fig. 4. Supersynoptic map of the large-scale radial magnetic field reconstructed from the odd zonal harmonics l = 1, 3, 5 smoothed over three Carrington rotations (upper panel) and from the odd zonal harmonics l = 5, 7, 9 smoothed over three Carrington rotations (lower panel) The map is taken from Obridko et al. (2023b) and reconstructed, magnetic field is given in G.

4. Equatorward wave

Another point is that the poleward waves are not directly related to the equatorward wave, which generates spots. The latter starts at much lower latitudes (40°–50°), although its sign coincides with one of the polar waves.

In fact, the polar and equatorial waves that arise in a common physical process are also not directly related. Moreover, they genetically consist of objects of different spatial structure. This is shown in the figure from Obridko et al. (2023b) (Fig. 4, lower panel). In order to ascertain the role of these waves, we have expanded the solar magnetic field into spherical harmonics. Data on the field longitudinal component obtained at the John Wilcox Observatory are available at the WEB site http://wso.stanford.edu/forms/prsyn.html. They are presented in the form of synoptic maps for each Carrington rotation based on individual observations for each day. The map is a table of the longitudinal magnetic field values taken at every five degrees of longitude at 30 points in equal steps of sine latitude from +14.5/15 to −14.5/15.

These data are used to calculate the coefficients of the multipole expansion under the assumption of a potential field (for more details, see Obridko et al., 2023b). Then, the supersynoptic map is recalculated for the entire observation interval.

The upper panel in Fig. 4 represents a supersynoptic map of the large-scale radial magnetic field reconstructed from three first odd zonal harmonics (l = 1, 3, 5) smoothed over three Carrington rotations. The map shows two waves directed poleward. However, the waves propagating towards the equator are less clearly pronounced; only some of their traces are visible on the plot. The lower panel shows for comparison the supersynoptic map of the large-scale radial magnetic field reconstructed only from three odd zonal harmonics (l = 5, 7, 9), also smoothed over three Carrington rotations. The map differs significantly from the previous one. No Rush-to-the-Poles effect is present, but the drift towards the equator is clearly pronounced. In summary, we can say that shortly before the inversion of the polar magnetic field on the photosphere, both large- and relatively small-scale magnetic fields appear almost simultaneously. However, once appearing, the fields begin to behave differently. The unipolar large-scale component propagates, creating the Rush-to-the-Pole effect. As a result, one can see that two rush-to-the-pole waves of opposite polarity propagate simultaneously on the solar surface. In contrast, the local magnetic fields are bipolar features that propagate to the equator.

To clarify the cyclic variation of the equatorial wave, we plotted the magnetic field averaged over a rotation for several latitudes separately for the northern hemispheres (Fig. 5). No additional assumptions were made. We used direct observations of the longitudinal field, as given on the Web site http://wso.stanford.edu/forms/Prsyn.html. The lower panel shows the total sunspot numbers in two hemispheres. Our analysis here is performed based on WSO data, and comparison with different magnetic field datasets such as NSO, HMI being obviously important (c.f. e.g. Riley et al., 2013) however, requires separate research. The SOHO/HMI and SOHO/MDI data cover a very short time interval and were obtained with a significantly higher spatial resolution.

On the topmost (near-polar) line, the magnetic field extrema are in antiphase with sunspot numbers as should be the case according to the basic dynamo model. The magnetic field extrema, both positive and negative, strictly correspond to the sunspot minima and the dates of the reversals are close to the moments of the sunspot maxima. But starting from the latitude of 50°, the situation changes. Now, the extrema correspond to the sunspot numbers. A wave independent of the polar zone and going to the equator has emerged.

Since the sunspot number does not depend on the sign of the mean field, we had to make a comparison with the time and latitude variations in the mean-field absolute value. This comparison is shown in Fig. 6. Here, one can readily see a secular decline in the near-polar magnetic field.

The maximum of the mean field in the period from 2004 to 2008, which should have corresponded to the prolonged decline phase of Cycle 23, is scarcely noticeable. Many observers noted the unusual character and long duration of this phase. At mid-latitudes, however, this feature disappears. The maximum at these latitudes and directly at the equator agrees with the secondary maximum of sunspot numbers. Note that even directly at the equatorial latitudes the mean magnetic field does not fully correspond to the sunspot curve. Transformation of the magnetic field into a sunspot is not straightforward and requires additional conditions.

5. Discussion

The mean field and the sunspots are closely related but not identical phenomena. The general idea is that the mean-field dynamo creates a mean-field toroidal flow, which, by means of some additional mechanism, disintegrates into separate tubes.

The mean magnetic flux forms magnetic fields of active regions and spots. We emphasize that this is not part of the dynamo process, and no new total flux is generated. This is a fairly complex process, the initial impulse of which is an increase in the magnetic field to a certain threshold value. At this value, the heat influx from below becomes weaker, and thermodynamic processes begin to act. If the region of the increased field is large enough compared to the horizontal optical thickness at the photosphere level, a dark feature (a sunspot) appears.

Helioseismic studies have shown that the most significant changes in the solar cycle occur in the Near-Surface Shear Layer (NSSL), which occupies about 5% of the solar radius at the top of the convection zone. The shear of velocity can transform part of the poloidal magnetic field into a toroidal one, and, in addition to the global dynamo operating in the main part of the convection zone, e.g. Pipin et al. (2023), the magneto-rotational instability may play a certain role (Vasil et al., 2024).

Even more complex is the variation in the radial gradient $d\log\omega/d\log r$ with latitude, depth, and formation time of sunspots and active

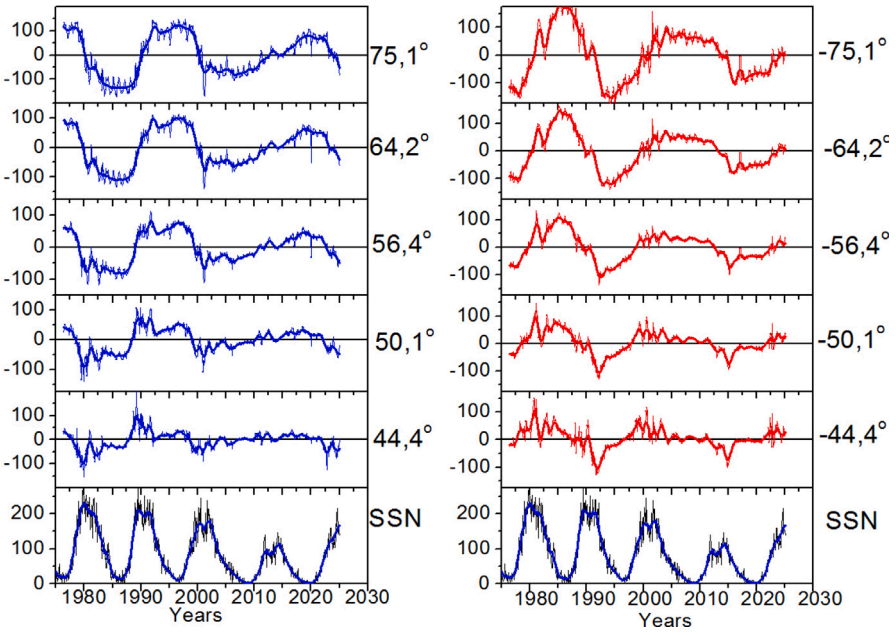

Fig. 5. Magnetic field averaged over a rotation for several latitudes separately for the northern (left panel) and southern (right panel) hemispheres. Panels in the lower row show for comparison SSN for both hemispheres together are identical for both columns.

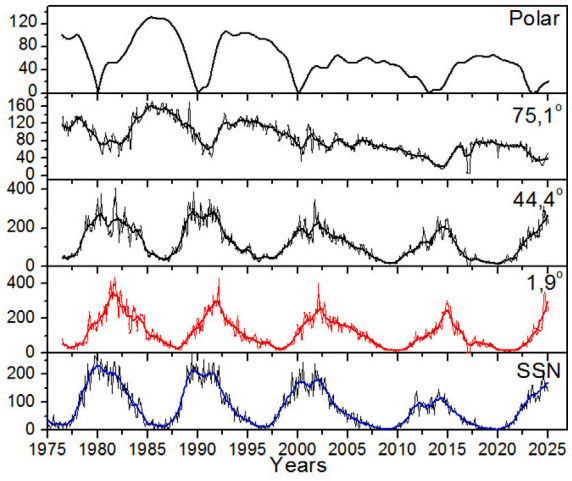

Fig. 6. Comparison in the mean-field absolute value and sunspot number.

regions in the leptocline — a shallow and sharp rotational shear layer at a depth of about 8 Mm (Rozelot et al., 2025; Kosovichev et al., 2025).

Below the leptocline, the negative gradient increases during an activity cycle in regions of strong magnetic field drifting towards the equator and decreases at high latitudes. In the leptocline, the variations are less pronounced and have a more complex structure similar to extended overlapping cycles of torsional oscillations. In particular, the rotational gradient is stronger not only during the maximum but also during the minimum of solar activity, when there are no strong magnetic fields on the solar surface.

In general, we can say that the mean-field dynamo is, undoubtedly, the main mechanism generating the solar activity and the 11-year cycle. However, the magnetic flux generated by the dynamo, being genetically the basis of solar activity, still does not allow us to conclude that there is an unambiguous connection between the characteristics of the magnetic field and other indices of solar activity, including the best-known index - the sunspot number. Therefore, a completely reliable long-term SSN forecast is possible only after the equatorial wave appears approximately 18 months before the maximum (note that this point was mentioned by Kleeorin et al. (2024)).

As a result of a complex combination of several interacting processes, Kleeorin et al. (2024) issued a reliable forecast for Cycle 25, which has not yet been completed. They created a dynamo model of the Sun that can reliably reproduce the properties of the mean field. The magnetic fields of active regions and spots are formed from the mean magnetic flux based on the NEMPI mechanism (e.g. Brandenburg et al., 2016, negative effective magnetic pressure effect). Its most important properties are the threshold nature and the conservation of the full flux. To predict solar activity over a short time interval, two approaches to the numerical solution of the problem are combined: the nonlinear mean-field dynamo equation and an artificial neural network.

We note that the shape of solar cycle in form of polar- and equatorward propagating activity wave looks to some extent similar to the form of stellar butterfly diagram suggested by Berdyugina and Henry (2007) for HR 1099.

CRediT authorship contribution statement

Vladimir Obridko: Investigation, Data curation, Conceptualization. **Antonina Shibalova:** Formal analysis, Data curation. **Dmitry Sokoloff:** Investigation, Conceptualization. **Ilya Livshits:** Formal analysis.

Funding

No founding to declare.

Acknowledgments

We thank T.Hoeksema for the solar magnetic field data.

Declaration of competing interest

The authors declare that they have no known competing financial interests or personal relationships that could have appeared to influence the work reported in this paper.

Data availability

All data on photospheric magnetic fields are available at http://wso.stanford.edu/synopticl.html and sunspot data from the World Data Center SILSO, Royal Observatory of Belgium, Brussels. Version V2.

References

Berdyugina, S.V., Henry, G.W., 2007. Butterfly diagram and activity cycles in HR 1099. Astrophys. J. 659, L157–L160. http://dx.doi.org/10.1086/517881, arXiv:astro-ph/0703530 [astro-ph].

Bhowmik, P., Jiang, J., Upton, L., Lemerle, A., Nandy, D., 2023. Physical models for solar cycle predictions. Space. Sci. Rev. 219, 40. http://dx.doi.org/10.1007/s11214-023-00983-x, arXiv:2303.12648 [astro-ph.SR].

Bhowmik, P., Nandy, D., 2018. Prediction of the strength and timing of sunspot cycle 25 reveal decadal-scale space environmental conditions. Nat. Commun. 9, 5209. http://dx.doi.org/10.1038/s41467-018-07690-0, arXiv:1909.04537 [astro-ph.SR].

Biswas, A., Karak, B.B., Kumar, P., 2023. Exploring the reliability of polar field rise rate as a precursor for an early prediction of solar cycle. Mon. Not. R. Astron. Soc. 526, 3994–4003. http://dx.doi.org/10.1093/mnras/stad2966, arXiv:2308.01155 [astro-ph.SR].

Brandenburg, A., Rogachevskii, I., Kleeorin, N., 2016. Magnetic concentrations in stratified turbulence: the negative effective magnetic pressure instability. New J. Phys. 18 (12), 125011. http://dx.doi.org/10.1088/1367-2630/aa513e, arXiv:1610.03459 [astro-ph.SR].

Bushby, P.J., Tobias, S.M., 2007. On predicting the solar cycle using mean-field models. Astrophys. J. 661, 1289–1296. http://dx.doi.org/10.1086/516628, arXiv:0704.2345 [astro-ph].

Choudhuri, A.R., Chatterjee, P., Jiang, J., 2007. Predicting solar cycle 24 with a solar dynamo model. Phys. Rev. Lett. 98, 131103. http://dx.doi.org/10.1103/PhysRevLett.98.131103, arXiv:astro-ph/0701527 [astro-ph].

Dikpati, M., Gilman, P.A., 2006. Simulating and predicting solar cycles using a flux-transport dynamo. Astrophys. J. 649, 498–514. http://dx.doi.org/10.1086/506314.

Dikpati, M., de Toma, G., Gilman, P.A., 2006. Predicting the strength of solar cycle 24 using a flux-transport dynamo-based tool. Geophys. Res. Lett. 33 (L05102), http://dx.doi.org/10.1029/2005GL025221.

Guo, W., Jiang, J., Wang, J.X., 2021. A dynamo-based prediction of solar cycle 25. Sol. Phys. 296, 136. http://dx.doi.org/10.1007/s11207-021-01878-2, arXiv:2108.01412 [astro-ph.SR].

Jiang, J., Wang, J.X., Jiao, Q.R., Cao, J.B., 2018. Predictability of the solar cycle over one cycle. Astrophys. J. 863, 159. http://dx.doi.org/10.3847/1538-4357/aad197, arXiv:1807.01543 [astro-ph.SR].

Jiang, J., Zhang, Z., Petrovay, K., 2023. Comparison of physics-based prediction models of solar cycle 25. J. Atmos. Sol.-Terr. Phys. 243, 106018. http://dx.doi.org/10.1016/j.jastp.2023.106018, arXiv:2212.01158 [astro-ph.SR].

Kitiashvili, I.N., 2016. Data assimilation approach for forecast of solar activity cycles. Astrophys. J. 831, 15. http://dx.doi.org/10.3847/0004-637X/831/1/15.

Kitiashvili, I., Kosovichev, A.G., 2008. Application of data assimilation method for predicting solar cycles. Astrophys. J. 688 (L49), http://dx.doi.org/10.1086/594999, arXiv:0807.3284 [astro-ph].

Kitiashvili, I.N., Kosovichev, A.G., 2011. Modeling and prediction of solar cycles using data assimilation methods. In: Rozelot, J.P., Neiner, C. (Eds.), In: Lecture Notes in Physics, vol. 832, Berlin Springer Verlag, p. 121. http://dx.doi.org/10.1007/978-3-642-19928-8_3.

Kleeorin, N., Kuzanyan, K., Safiullin, N., Rogachevskii, I., Obridko, V., Porshnev, S., Stepanov, R., 2024. Forecast of solar activity based on mean-field dynamo model and neural network. Astron. Astrophys. Trans. 34, 371–388. http://dx.doi.org/10.48550/arXiv.2411.10380, arXiv:2411.10380 [astro-ph.SR].

Kosovichev, A.G., Basu, S., Bekki, Y., et al., 2025. Structure and dynamics of the sun's interior revealed by the helioseismic and magnetic imager. Sol. Phys. 300, 70. http://dx.doi.org/10.1007/s11207-025-02480-6, arXiv:2503.07880 [astro-ph.SR].

Labonville, F., Charbonneau, P., Lemerle, A., 2019. A dynamo-based forecast of solar cycle 25. Sol. Phys. 294, 82. http://dx.doi.org/10.1007/s11207-019-1480-0.

McIntosh, S.W., Chapman, S., Leamon, R.J., et al., 2020. Overlapping magnetic activity cycles and the sunspot number: Forecasting sunspot cycle 25 amplitude. Sol. Phys. 295, 163. http://dx.doi.org/10.1007/s11207-020-01723-y, arXiv:2006.15263 [astro-ph.SR].

McIntosh, S.W., Leamon, R.J., Egeland, R., et al., 2019. What the sudden death of solar cycles can tell us about the nature of the solar interior. Sol. Phys. 294, 88. http://dx.doi.org/10.1007/s11207-019-1474-y, arXiv:1901.09083 [astro-ph.SR].

McIntosh, S.W., Leamon, R.J., Egeland, R., et al., 2021. Deciphering solar magnetic activity: 140 years of the 'extended solar cycle' - mapping the hale cycle. Sol. Phys. 296, 189. http://dx.doi.org/10.1007/s11207-021-01938-7, arXiv:2010.06048 [astro-ph.SR].

McIntosh, S.W., Wang, X., Leamon, R.J., et al., 2014. Deciphering solar magnetic activity. I. On the relationship between the sunspot cycle and the evolution of small magnetic features. Astrophys. J. 792, 12. http://dx.doi.org/10.1088/0004-637X/792/1/12, arXiv:1403.3071 [astro-ph.SR].

Mininni, P.D., Gómez, D.O., Mindlin, G.B., 2002. Biorthogonal decomposition techniques unveil the nature of the irregularities observed in the solar cycle. Phys. Rev. Lett. 89, 061101. http://dx.doi.org/10.1103/PhysRevLett.89.061101.

Nandy, D., 2021. Progress in solar cycle predictions: Sunspot cycles 24-25 in perspective. Sol. Phys. 296, 54. http://dx.doi.org/10.1007/s11207-021-01797-2, arXiv:2009.01908 [astro-ph.SR].

Obridko, V.N., Shibalova, A.S., Sokoloff, D.D., 2023b. The extended solar cycle and asymmetry of the large-scale magnetic field. Mon. Not. R. Astron. Soc. 523, 982–990. http://dx.doi.org/10.1093/mnras/stad1515, arXiv:2305.19427 [astro-ph.SR].

Obridko, V., Sokoloff, D., Katsova, M., 2023a. Estimates of the height and date of the 25th cycle of solar activity. Astron. Tsirkulyar 1658, 1. http://dx.doi.org/10.24412/0236-2457-2023-1658-1-4, arXiv:2307.05725 [astro-ph.SR].

Petrovay, K., 2020. Solar cycle prediction. Living Rev. Sol. Phys. 17, 2. http://dx.doi.org/10.1007/s41116-020-0022-z, arXiv:1907.02107 [astro-ph.SR].

Pipin, V.V., Kosovichev, A.G., Tomin, V.E., 2023. Effects of emerging Bipolar Magnetic Regions in mean-field dynamo model of solar cycles 23 and 24. Astrophys. J. 949, 7. http://dx.doi.org/10.3847/1538-4357/acaf69, arXiv:2210.08764 [astro-ph.SR].

Riley, P., Linker, J.A., Mikić, Z., 2013. On the application of ensemble modeling techniques to improve ambient solar wind models. J. Geophys. Res. (Space Phys.) 118, 600–607. http://dx.doi.org/10.1002/jgra.50156.

Rozelot, J.P., Kosovichev, A., Kitiashvili, I., 2025. Improving our knowledge of the solar near-surface shear layer: The special case of the leptocline. http://dx.doi.org/10.48550/arXiv.2501.08021, arXiv e-prints, arXiv:2501.08021 [astro-ph.SR].

Upton, L.A., Hathaway, D.H., 2018. An updated solar cycle 25 prediction with AFT: The modern minimum. Geophys. Res. Lett. 45, 8091–8095. http://dx.doi.org/10.1029/2018GL078387, arXiv:1808.04868 [astro-ph.SR].

Vasil, G.M., Lecoanet, D., Augustson, K., et al., 2024. The solar dynamo begins near the surface. nat. 629, 769–772. http://dx.doi.org/10.1038/s41586-024-07315-1, arXiv:2404.07740 [astro-ph.SR].

Wang, Y.M., Sheeley, N.R., 2009. Understanding the geomagnetic precursor of the solar cycle. Astrophys. J. Lett. 694, L11–L15. http://dx.doi.org/10.1088/0004-637X/694/1/L11.